Biogeosciences Discuss., 11, 14063–14096, 2014
www.biogeosciences-discuss.net/11/14063/2014/
doi:10.5194/bgd-11-14063-2014

Biogeosciences Discussions
Open Access

Spatial and temporal dynamics of CO_2 partial pressure in the Yellow River, China

L. Ran[1], X. X. Lu[1,2], J. E. Richey[3], H. Sun[4], J. Han[4], R. Yu[2], S. Liao[5], and Q. Yi[6]

[1]Department of Geography, National University of Singapore, 117570, Singapore
[2]College of Environment & Resources, Inner Mongolia University, Hohhot, 010021, China
[3]School of Oceanography, University of Washington, Box 355351, Seattle, WA, 98195-5351, USA
[4]Institute of Geology and Geophysics, Chinese Academy of Sciences, Beijing, 100029, China
[5]Tongguan Hydrographic Station, Yellow River Conservancy Commission, Tongguan, 714399, China
[6]Toudaoguai Hydrographic Station, Yellow River Conservancy Commission, Baotou, 014014, China

Received: 2 September 2014 – Accepted: 22 September 2014 – Published: 2 October 2014

Correspondence to: X. X. Lu (geoluxx@nus.edu.sg)

Published by Copernicus Publications on behalf of the European Geosciences Union.

Abstract

Carbon transport in river systems is an important component of the global carbon cycle. Most rivers of the world act as atmospheric CO_2 sources due to high riverine CO_2 partial pressure (pCO_2). We investigated the pCO_2 dynamics in the Yellow River watershed by using historical water chemistry records (1950s–1984) and recent sampling along the mainstem (2011–2012). Except the headwater region where the pCO_2 was lower than the atmospheric equilibrium (i.e., 380 µatm), river waters in the remaining watershed were supersaturated with CO_2. The average pCO_2 for the watershed was estimated at 2810 ± 1985 µatm, which is 7-fold the atmospheric equilibrium. This indicates a strong CO_2 outgassing across the water-air interface. As a result of severe soil erosion and dry climate, waters from the Loess Plateau in the middle reaches had higher pCO_2 than that from the upper and lower reaches. From a seasonal perspective, the pCO_2 varied from about 200 µatm to > 30 000 µatm with higher pCO_2 usually occurring in the dry season and low pCO_2 in the wet season (at 73 % of the sampling sites), suggesting the dilution effect of water. While the pCO_2 responded positively to total suspended solids (TSS) transport when the TSS was less than 100 kg m^{-3}, it slightly decreased and remained stable when the TSS exceeded 100 kg m^{-3}. This stable pCO_2 is largely due to gully erosion that mobilizes subsoils characterized by low organic matter for decomposition. In addition, human activities have changed the pCO_2 dynamics. Particularly, flow regulation by dams can diversely affect the temporal changes of pCO_2, depending on the physiochemical properties of the regulated waters and adopted operation scheme. Given the high pCO_2 in the Yellow River waters, the resultant CO_2 outgassing is expected to be substantial and warrants further investigation.

BGD
11, 14063–14096, 2014

1 Introduction

Rivers play a crucial role in the global carbon cycle, because they can modulate the carbon dynamics not only of the watersheds but also of the coastal systems into which river waters are discharged. Fluvial carbon export represents an important pathway linking land and the ocean. Approximately 0.9 Gt of carbon is delivered into the oceans per year via inland waters (Battin et al., 2009; Cole et al., 2007). However, rivers are not merely passive conduits that shuttle carbon from land to sea. Evidence is accruing to indicate that, while only a small portion of carbon that enters a river network finally reaches the ocean, a considerable fraction would be buried in sedimentary deposits or returned to the atmosphere en route (Cole et al., 2007; Richey et al., 2002; Yao et al., 2007). Consequently, rivers are viewed as sources of atmospheric CO_2. Recent estimates show that global inland waters can transfer 0.75–2.1 Gt C yr^{-1} into the atmosphere (Cole et al., 2007; Aufdenkampe et al., 2011; Tranvik et al., 2009; Raymond et al., 2013). Comparative studies associated with horizontal carbon fluxes have highlighted the significance of CO_2 evasion in assessing global carbon budget (Cole et al., 2007; Richey et al., 2002). With such a huge efflux, the terrestrial CO_2 sink may prove smaller than previously thought (Melack, 2011).

Riverine CO_2 originates primarily from soil respiration and decomposition of organic matter. As an important parameter in estimating CO_2 outgassing, its partial pressure (pCO_2) indicates the CO_2 concentration in rivers and the gradient relative to the atmospheric equilibrium (i.e., 380 µatm). Most rivers of the world tend to have significantly higher pCO_2 than the atmospheric equilibrium, suggesting a great emission potential (Cole et al., 2007; Striegl et al., 2012). While the riverine pCO_2 dynamics of mainstem or estuary waters have been widely recognized, such as the Amazon (Richey et al., 2002), Pearl (Yao et al., 2007), and Columbia (Evans et al., 2013), a holistic assessment of pCO_2 concerning a complete river network is rare. This is largely caused by the constraints of time and logistics to conduct spatial sampling covering not only the mainstem but also the lower stream-order tributaries. Indeed, tributaries are more bio-

BGD
11, 14063–14096, 2014

geochemically active because they have stronger turbulence and more rapid mixing with the atmosphere than the mainstem (Alin et al., 2011; Benstead and Leigh, 2012; Butman and Raymond, 2011). For example, Aufdenkampe et al. (2011) found the CO_2 outgassing fluxes from small streams could be 2–3 times higher than from larger rivers. Thus, estimating CO_2 outgassing based only on the mainstem will underestimate the total emission flux of a specific river system. Analyzing pCO_2 dynamics through high-resolution sampling at space and time scales is a prerequisite for precisely evaluating CO_2 outgassing and its implications for carbon cycle.

The Yellow River is characterized by high sediment and total dissolved solids (TDS) among the world's large rivers. Its TDS concentration of 452 mg L^{-1} is about four times the world median value (Chen et al., 2005). Based on measurements at hydrological gauges or in specific river reaches, prior studies have investigated its chemical weathering and organic carbon transport (e.g., Zhang et al., 1995; Wu et al., 2008; Wang et al., 2012; Ran et al., 2013). Hillslope ecosystem respiration and the impact of land use change on carbon storage have also been analyzed (Zhao et al., 2008; Li et al., 2010). By contrast, few studies have examined its carbon dynamics in river waters and how riverine pCO_2 has responded to catchment features. Using historical records across the Yellow River watershed during the period 1950s–1984 and recent sampling along the mainstem, this study aimed to investigate the spatial and temporal variations of its riverine pCO_2 and its responses to natural and human factors.

2 Materials and methods

2.1 Site description

The Yellow River drains 752 000 km^2 of north China, originating in the Tibetan Plateau and flowing eastward into the Bohai Sea (Fig. 1). Located in a semiarid-arid climate, its precipitation is spatially highly variable, decreasing from 700 mm yr^{-1} in the southeast to 250 mm yr^{-1} in the northwest (Zhao, 1996). Likewise, temperature changes signifi-

BGD
11, 14063–14096, 2014

cantly, with the mean temperature in the upper (above Toudaoguai), middle (approximately between Toudaoguai and the Xiaolangdi Dam), and lower (below the Xiaolangdi Dam) reaches being 1–8, 8–14, and 12–14 °C, respectively (Chen et al., 2005). Because the Yellow River basin is in large part surrounded by the Loess Plateau that has typically accumulated huge erodible loess deposits (Fig. 1), it suffers from severe soil erosion. Approximately 1.6 Gt of sediment was transported to the ocean per year prior to the 1970s (Syvitski et al., 2005). For comparison, the mean water discharge was only 49 $km^3\,yr^{-1}$ (Zhao, 1996).

Both hydrological regime and landscape within the watershed have been greatly altered due to intensive human activity (Ran and Lu, 2012). While the water discharge has dropped to 15 $km^3\,yr^{-1}$ during the recent decade, the sediment flux has decreased to about 0.14 $Gt\,yr^{-1}$ as a result of massive soil conservation and sediment trapping by dams. Among the numerous dams, these constructed on the mainstem channel play fundamental roles in regulating delivery of water, sediment, and dissolved solids (Ran and Lu, 2012), especially the joint operation of the Sanmenxia and Xiaolangdi dams since 2000. With about 140 million people currently residing within the watershed, the population density is 180 person km^{-2} (Chen et al., 2005), and it exceeds 300 person km^{-2} in some agricultural areas in the middle reaches. Consequently, land use has become increasingly both extensive and intensive.

The Yellow River basin was mainly developed on the Sino-Korean Shield with Quaternary loess deposits overlying the vast middle reaches and Archean to Tertiary granites and metamorphic rocks in areas near the basin boundaries and in the lower reaches (Chen et al., 2005). Chemical analyses of loess samples show that feldspar, micas, and quartz are the most common detrital minerals with carbonates accounting for 10–20 % (Zhang et al., 1995). Because the loess deposits cover about 46 % of the total drainage area, the river presents high alkalinity and intense chemical weathering. With exceptionally high TDS concentration the Yellow River delivers around 11 Mt of dissolved solids per year to the Bohai Sea (Gaillardet et al., 1999).

BGD
11, 14063–14096, 2014

2.2 Historical records of water chemistry

Historical records of major ions measured from a hydrological monitoring network were extracted from the Yellow River Hydrological Yearbooks, which are yearly produced by the Yellow River Conservancy Commission (YRCC). Other variables concurrently measured at each sampling event, including pH, water temperature, water discharge, and total suspended solids (TSS), were also retrieved from the yearbooks for this study. Over the period from the 1950s to 1984, the sampling frequency ranged from 1 to 5 times per month, depending on hydrological regime. Sampling at some stations during the period 1966–1975 were suspended or completely stopped due to political chaos. Post-1984 records are not in the public domain. Given the discontinuity in sampling, only the stations with at least 6 samples in a year were analyzed. A total of 129 stations with 15 029 water chemistry measurements were compiled (Fig. 1).

Chemical analyses of the collected water samples were performed under the authority of the YRCC following the standard procedures and methods described by Alekin et al. (1973) and the American Public Health Association (1985). The pH and temperature were measured in field, and total alkalinity (TAlk) was determined using a fixed end-point titration method. Detailed description of the sampling and analysis procedures can be found in Chen et al. (2002a). The results were summarized in Supporting Information.

Use of historical records always raises the issue of data reliability. No detailed information on quality assurance and quality control is available in the hydrological reports. Extensive efforts have been made to assess the data quality by analyzing the parameter differences measured at the same station but by different agencies. The Luokou station on the lower Yellow River mainstem has been monitored under the United Nations Global Environment Monitoring System (GEMS) Water Programme since 1980 (only yearly means available at http://www.unep.org/gemswater). As pCO_2 is considerably sensitive to pH changes (Li et al., 2012), the pH values from the two sources were compared (Table 1), which showed that the dataset from the Hydrological Year-

BGD
11, 14063–14096, 2014

books agreed well with the GEMS/Water Programme dataset with differences of < 2 %. The high data quality of the hydrological reports can also be confirmed through the concentration comparison of major ions in the two datasets (c.f., Chen et al., 2005).

Given the data paucity for the upper Yellow River, data collected at 17 sites in the headwater region were retrieved from Wu et al. (2005) (Fig. 1; Supplement). They measured pH and temperature along the mainstem and major tributaries and determined the TAlk through Gran titration. Comparison with previous sampling results (Zhang et al., 1995) showed their data agreed well.

2.3 Recent field sampling

From July 2011 to July 2012, weekly sampling on the mainstem was undertaken at Toudaoguai, Tongguan, and Lijin stations (Fig. 1; Supplement). The frequency increased (i.e., daily) when large floods occurred. Water column samples were collected ~ 0.5 m below the surface water and kept in acid-washed, but carefully neutralized, high density polyethylene containers. Determination of pH and water temperature was performed in situ using a Hanna HI9125 pH meter, which was calibrated prior to each measurement against pH7.01 and pH10.01 buffers. Replicate measurements showed the precision for pH and temperature were ±0.04 units and ±0.1 °C, respectively. The TAlk was determined by titrating 50 mL filtered water through 47 mm Whatman GF/F filters (0.7 µm pore size) with 0.02 M HCl solution within 5 h after sampling. Three parallel titrations showed the analytical error was below 3 %. The parallel alkalinity results were then averaged. In total, 163 samples were collected. Ancillary data, including daily water discharge and TSS, were acquired from the YRCC. Generally, the sampling results at Toudaoguai and Tongguan reflect the TAlk and pCO_2 changes on the Loess Plateau, while the Lijin measurements represent seaward export as it is located 110 km upstream of the river mouth and free of tidal influences.

BGD
11, 14063–14096, 2014

2.4 Calculations of DIC species and pCO_2

Total dissolved inorganic carbon (DIC) species in river systems, including HCO_3^-, CO_3^{2-}, H_2CO_3, and aqueous CO_2 (CO_{2aq}), are in temperature- and pH-dependent equilibrium with another, such as the equilibrium between atmosphere CO_2 and aqueous CO_2 (Li et al., 2012). DIC species can be determined by the Henry's Law, from which the pCO_2 can be calculated using the CO2SYS program (Lewis and Wallace, 1998).

$$CO_2 + H_2O \leftrightarrow H_2CO_3^* \leftrightarrow H^+ + HCO_3^- \leftrightarrow 2H^+ + CO_3^{2-} \quad (1)$$

$$K_{CO_2} = [H_2CO_3^*]/[pCO_2] \quad (2)$$

$$K_1 = [H^+][HCO_3^-]/[H_2CO_3^*] \quad (3)$$

$$K_2 = [H^+][CO_3^{2-}]/[HCO_3^-] \quad (4)$$

where, $H_2CO_3^*$ is the sum of CO_{2aq} and the true H_2CO_3, K_i are temperature (T) dependant dissociation constants between DIC species (Clark and Fritz, 1997):

$$pK_{CO_2} = -7 \times 10^{-5}T^2 + 0.016T + 1.11 \quad (5)$$

$$pK_1 = 1.1 \times 10^{-4}T^2 - 0.012T + 6.58 \quad (6)$$

$$pK_2 = 9 \times 10^{-5}T^2 - 0.0137T + 10.62 \quad (7)$$

where, $pK = -\lg K$.

Then, the pCO_2 can be simply expressed as:

$$pCO_2 = [H_2CO_3^*]/K_{CO_2} = [H^+][HCO_3^-]/K_{CO_2}K_1 \quad (8)$$

With the pH mostly ranging from 7.4 to 8.5 indicative of natural processes in the river, HCO_3^- is considered equivalent to alkalinity because it accounts for > 96 % of the TAlk. This approach has been frequently used and demonstrated high riverine pCO_2 in Chinese river systems (e.g., Yao et al., 2007; Li et al., 2012). To validate the simplification,

BGD
11, 14063–14096, 2014

we also calculated the DIC species and pCO_2 using the program PHREEQC (Hunt et al., 2011). The pCO_2 results derived by PHREEQC were very close to that returned by CO2SYS with < 3 % differences.

3 Results

3.1 Characteristics of hydrochemical setting

To better investigate the spatial changes of hydrochemical variables, the watershed was divided into seven sub-basins: the headwater region (HR), the Huang-Tao tributaries (HT), the Qing-Zuli tributaries (QZ), the Ning-Meng reaches (NM), the Wei-Yiluo tributaries (WY), the middle reaches (MY), and the lower reaches (LY) (Fig. 2). The Yellow River waters were characterized by high alkalinity with the pH presenting significant spatial variations (Fig. 2a). While high pH values were mostly observed in the headwater region where the highest was 9.1, relatively low pH (i.e., < 7.71) was recorded at the QZ tributary sites with the lowest being 6.4. For the waters from the Loess Plateau, the pH was in the range of 7.71–8.47. Towards the river mouth, it showed a downward trend in the lower reaches (LY). With one exception at Lijin (Fig. 1), the pH values were all below 8.13 and even below 7 at some tributary sites. In addition to spatial variations, it showed considerable seasonal changes. As exemplified in Fig. 3a, the waters were generally more alkaline in the dry season (October–May) than in the wet season (June–September).

Similarly, with a range of 855–8633 µmol L^{-1}, the TAlk presented complex spatial variability throughout the watershed. While the HR and LY sub-basins showed the lowest TAlk (< 2600 µmol L^{-1}), the sub-basins on the Loess Plateau had considerably high alkalinity with a mean TAlk of about 3800 µmol L^{-1}. The highest TAlk (8633 µmol L^{-1}) was measured in the QZ sub-basin. It is evident that the TAlk and pH showed similar spatial variations, but in the reverse direction with high TAlk coinciding with low pH. With regard to all the sampling results, about 58 % of the TAlk values fell into the range

BGD
11, 14063–14096, 2014

of 3000–4000 µmol L^{-1} and 92 % into the range of 2000–5000 µmol L^{-1}. For the whole Yellow River watershed, its mean TAlk was 3665 ± 988 µmol L^{-1}. In addition, its TAlk remained largely stable during the sampling period. Figure 3b shows an example of the TAlk changes at Luokou. Despite the discontinuous measurement from 1968 to 1974, the TAlk did not change significantly over time.

3.2 Spatial and temporal variability of pCO_2

The pCO_2 varied significantly throughout the watershed with two orders of magnitude from ~ 200 µatm to more than 30 000 µatm. Except the headwater region that showed lower pCO_2 than the atmospheric equilibrium, the remaining watershed had a considerably high pCO_2 (Fig. 2b). The highest pCO_2 was 36 790 µatm estimated at a tributary site in the QZ sub-basin resulting from low pH and high TAlk. For the middle Yellow River basin, including the MY and WY sub-basins, the waters were considerably supersaturated with CO_2 with the pCO_2 ranging from 1000 to 5000 µatm (Fig. 2b). Moreover, the pCO_2 level in the lower Yellow River reaches (LY) was much higher and can exceed 10 000 µatm. On average, the pCO_2 in the Yellow River watershed was 2810 ± 1985 µatm, 7-fold the atmospheric CO_2 equilibrium. It must be recognized however that, unlike the historical dataset that was monthly measured, sampling in the headwater region by Wu et al. (2005) was conducted only during the late May and June of 1999 and 2000 when the wet season had barely started. Given the flushing effect of infiltrating rainfall and snowmelt flows at the beginning of wet season (Melack, 2011; Clow and Drever, 1996), the resultant TAlk and pCO_2 are expected to be close to highest.

With a positive correlation with TAlk, the pCO_2 level at most sampling sites also showed strong seasonal variations. At 73 % of the sampling sites, higher pCO_2 occurred in the months before the onset of the wet season. During the wet season, it decreased to a relatively low level before going up again from October onwards. The seasonal ratio of pCO_2, defined as the ratio of pCO_2 in the dry season over that in the wet

BGD
11, 14063–14096, 2014

season, ranged from 0.8 to 2.3 with > 55 % ratios between 0.9 and 1.5. To more clearly show its spatial and temporal changes, Fig. 4 plots the high temporal-resolution sampling results at Toudaoguai, Tongguan, and Lijin. Both the TAlk and pCO_2 showed large spatial differences among the three sites. The mean TAlk at Tongguan (4075 µmol L^{-1}) was higher than at the upstream Toudaoguai and the downstream Lijin (3664 and 3622 µmol L^{-1}, respectively). Likewise, the mean pCO_2 at Tongguan (4770 µatm) was about 3 and 3.5 times that at Toudaoguai (1624 µatm) and Lijin (1348 µatm), respectively (see Supplement). The highest pCO_2 of 26 318 µatm was estimated at Tongguan in early May.

When compared with tributaries, the mainstem exhibited more complicated seasonal patterns (Fig. 4). The TAlk was higher in the dry season than in the wet season, in particular for Tongguan located downstream of the Loess Plateau (Table 2; Fig. 1). The pCO_2 showed similar seasonal variations. Contrast to the weak seasonal changes at Toudaoguai and Lijin, the pCO_2 at Tongguan in the dry season (6016 µatm on average) was twofold that in the wet season. It is clear the pCO_2 increased substantially in both seasons as waters from the Loess Plateau entered the mainstem, and then decreased along the channel course towards the ocean (Table 2). Furthermore, the pCO_2 presented complex relationships with water discharge. While the pCO_2 changed synchronously with water at Toudaoguai, it decreased with increasing water in the wet season at Tongguan and Lijin (Fig. 4). In general, the pCO_2 at all the three stations was significantly higher than the atmospheric equilibrium, though the pCO_2 differences between river waters and the atmosphere varied substantially between different stations or different seasons.

BGD
11, 14063–14096, 2014

4 Discussion

4.1 Environmental controls on riverine pCO_2

Total alkalinity of river waters reveals the buffering capacity of waters in a carbonate system to neutralize acids and bases. Due to abundant carbonate outcrops, groundwater in the Yellow River basin was highly alkaline (Chen et al., 2002b), which directly led to the higher TAlk in the dry season when baseflow constituted 90 % of the river runoff. High TAlk on the Loess Plateau was probably the result of chemical weathering. With the widespread carbonates in this region, chemical weathering of rocks and soils in the loess deposits has generated high dissolved solids with HCO_3^- being the dominant ion (Chen et al., 2005; Zhang et al., 1995).

Chen et al. (2005) analyzed the temporal variations of major dissolved solutes during 1958–2000, and found they showed persistent increasing trends due largely to human impacts. In contrast, the long-term stable TAlk (Fig. 3) indicated that it was not significantly affected. Natural weathering processes must have played a more important role in controlling the transport of DIC species and TAlk. Plotting TAlk with corresponding flow showed that they were negatively correlated (Fig. 5). However, the TAlk did not change at the same rate as water in the wet season. It decreased more slowly as revealed by the exponents in the inserted equations. Compared with the water changes, a narrower TAlk fluctuation suggested the coupling results of enhanced alkalinity export during the wet season and the dilution effect of water (Raymond and Cole, 2003; Piòol and Avila, 1992).

Riverine pCO_2 is an indicator of the internal carbon dynamics and external biogeochemical processes of terrestrial ecosystems within a catchment (Jones et al., 2003). Four main processes determining riverine pCO_2 are: (i) production and transport of soil CO_2, (ii) in situ respiration and decomposition of organic matter, (iii) aquatic photosynthesis; and (iv) CO_2 emission across the water-air interface (Yao et al., 2007; Richey, 2003). Evidently, the first two processes are able to increase the pCO_2, whereas the

BGD
11, 14063–14096, 2014

other two processes tend to reduce it. Whether river waters are supersaturated with CO_2 depends on the balance between these processes.

Carbon in river waters is largely derived from biogeochemical processes occurring in terrestrial ecosystems. Changes in terrestrial ecosystems will thus affect riverine carbon cycle. Because soil respiration and CO_2 production are highly dependent on temperature and rainfall (Shi et al., 2011; Hope et al., 2004; Epron et al., 1999), higher riverine pCO_2 is expected in the wet season due to soil CO_2 flushing. This is in contrast to the observed seasonal variations in the Yellow River. Unique precipitation distribution and hydrological regime may have contributed to these abnormal changes. The Yellow River basin is characteristic of high-intensity rainfalls; several storms in the wet season can account for > 70 % of the annual precipitation (Zhao, 1996). Coupled with its distinct soil surface microtopography with texture consisted mainly of silt and clay, Hortonian overland flow is the dominant runoff process (Liu and Singh, 2004). Without sufficient time for infiltration into deep soil horizons, the overland runoff generated by high-intensity rainfalls would have diluted the TAlk and reduced the riverine pCO_2.

With extremely high suspended solids, the Yellow River provides an excellent case study for understanding the responses of pCO_2 to TSS (Fig. 6). Based on measurements in the sediment yielding areas on the Loess Plateau, the pCO_2 increased exponentially with increasing TSS under low TSS scenarios. This reflects the soil erosion processes distinctive to the Loess Plateau (Zhao, 1996; Rustomji et al., 2008). At the initial stage of soil erosion, the surficial soils with abundant organic carbon are first eroded away by surface runoff into rivers. Decomposition of the labile organic carbon in the eroded soils will increase the riverine pCO_2. Thus, the pCO_2 responded positively to soil erosion and increasing TSS. This positive response lasted until the topsoils were completely eroded. When the TSS was higher than 100 kg m^{-3}, however, the pCO_2 decreased slightly and remained stable since then (Fig. 6). The threshold of ca. 100 kg m^{-3} is consistent with the commonly defined hyperconcentrated flows (Xu, 2002). Hyperconcentrated flows indicating TSS greater than 100 kg m^{-3} are frequently recorded in the Yellow River, in which gully erosion contributes > 50 % of the fluvial

BGD
11, 14063–14096, 2014

sediment loads (Ran et al., 2014). Compared with the organic carbon in the topsoils (usually 0.5–1.5 %), it is much lower in the subsoils (i.e., 0.2–0.3 %) and shows uniformity with depth (Zhang et al., 2012; Wang et al., 2010). The mobilized subsoils through gully erosion therefore have lower organic matter composition for decomposition, resulting in the reduced and stable pCO_2 regardless of the increasing TSS.

Lower pCO_2 in the headwater region was caused by relatively low TAlk and high pH. Statistical analyses showed that its TAlk was 25 % lower than the basin average while the pH 7 % higher. Compared to other sub-basins, the headwater region is covered by an alpine meadow ecosystem and experiences reduced soil erosion, which may have constrained the leaching of organic matter. Moreover, this sub-basin is in cold environments and its temperature falls below zero from October to March owing to high elevation (> 3000 m). Microbial decomposition of organic matter and ecosystem respiration are kinetically inhibited as affected by the low temperature (Kato et al., 2004), resulting in the low pCO_2. Unique climate also denotes the seasonal patterns of pCO_2 in the upper and middle Yellow River. Occurrence of the highest pCO_2 at Toudaoguai and Tongguan in March through May is likely controlled by ice-melt floods (Fig. 4a and b). In the coldest months, water surface in the northernmost reaches (between QTX and Toudaoguai; Fig. 1) freezes up until early spring (Chen and Ji, 2005). The aqueous CO_2 could not be efficiently released due to ice protection and typically accumulates below the ice cover. Starting from early spring, the ice begins to thaw and CO_2-laden waters are exported downstream to the sampling sites, probably causing the sharply increased pCO_2. Also, the lower temperature in the dry season would be responsible for the higher pCO_2 as the solubility of CO_2 increases with decreasing water temperature. More research is needed to elucidate these relationships.

High pCO_2 in the QZ sub-basin (Fig. 2b) was primarily the result of high TAlk due to its geological background. Its major rock types are carbonates, detritus (quartz and feldspar), and red-beds (gypsum and halite) (Zhang et al., 1995), which are highly vulnerable to weathering. Consequently, its mean TDS was 8–14 times the basin average (Chen et al., 2005). Some streams in this sub-basin are even nicknamed as

BGD
11, 14063–14096, 2014

"bitter streams" for their high TDS concentrations. Furthermore, this sub-basin has high drought index with its annual evaporation being > 8 times the annual precipitation (Chen et al., 2005). Such strong evaporation will result in not only the precipitation of minerals with low solubility (e.g., gypsum and halide), but the elevated concentrations of solutes not removed during the crystallization process. Another possible cause is the severe erosion due to sparse vegetation cover. In addition to mobilization of organic matter, soil erosion is able to enhance chemical weathering by increasing the exposure surface of fresh minerals to atmosphere (Millot et al., 2002). This would also contribute to greatly condensed DIC species in river waters and thus high pCO_2.

Downstream variations of TAlk and pCO_2 along the mainstem indicated that the waters from the Loess Plateau had higher TAlk and were more supersaturated with CO_2 than the upper and lower Yellow River waters (Fig. 7). As discussed earlier, severe soil erosion on the Loess Plateau may be the major reason. Moreover, low groundwater table in the arid climate allows deeper soil horizons to adequately interact with the atmosphere, which triggers chemical weathering and generates huge quantities of HCO_3^-. Increasing pCO_2 until Tongguan suggested the integrated responses of pCO_2 to these factors. Without large tributaries joining the lower Yellow River (Fig. 1), the decreasing TAlk and pCO_2 along the mainstem revealed reduced TAlk input. Overall, the spatial changes of TAlk and pCO_2 were the combined results of differences in soil property, hydrological regime, climate, and landform development.

4.2 Anthropogenic impacts on riverine pCO_2

Agriculture in the Yellow River basin has been conducted for more than 2000 years (Chen et al., 2005). Tilling practices can not only expand the exposure area of soil materials, but alter the hydrology of surficial soils, increasing the contact rate between water and minerals and thus the alkalinity export (Raymond and Cole, 2003). Dissolution of soil CO_2 and decomposition of organic matter in agricultural fields are also likely to boost alkalinity production. Furthermore, due to human-induced rainfall acidification, significant pH decreases in the middle and lower Yellow River basin have been widely

BGD
11, 14063–14096, 2014

detected (Guo et al., 2010). The decreased pH may have been partially responsible for the elevated pCO_2 in these regions relative to the headwater region that had higher pH (Fig. 2).

Differences in the hydrochemical parameters between historical records and recent sampling clearly revealed the temporal changes over the period. Significant increase in pH at Toudaoguai was largely caused by widespread salinization of agricultural soils. There are two large irrigation zones upstream of Toudaoguai; large quantities of water is diverted every year for desalination and irrigation (Chen et al., 2005). The diverted water volume has gradually increased since 1960 due to growing demand (Ran et al., 2014). When washed out from irrigated farmlands, the return water characterized by high pH caused the riverine pH to increase, leading further to greatly reduced pCO_2 despite the roughly stable TAlk (Fig. 3b). Particularly, it is worth noting that the magnitude of reduction was much higher in the wet season when the high-pH return water reached the mainstem with floods (Table 2).

Trapping of water and suspended solids by dams will alter river-borne carbon dynamics (Cole et al., 2007). That is because reduced flow turbulence and extended residence time will promote photosynthesis of aquatic plants and reduce aqueous CO_2 concentration (Raymond and Cole, 2001; Teodoru et al., 2009). Figure 8 presents an example of the impact of dams on downstream pCO_2 changes. Located on the upper mainstem channel (Fig. 1), operation of the Qingtongxia Dam since 1968 has substantially affected the pCO_2. Despite insignificant changes of the TAlk between the pre- and post-dam periods (Fig. 8), enhanced aquatic photosynthesis after dam operation owing to reduced TSS may have absorbed aqueous CO_2 and resulted in increased pH by shifting the chemical equilibrium of Eq. (1). Accordingly, the riverine pCO_2 declined during the post-dam period with the elevated pH and roughly stable TAlk.

For the dams on the Loess Plateau constructed mostly during 1960–2000, however, aqueous photosynthesis appears to be at a low level owing to its extremely high TSS concentration and limited light availability (Chen et al., 2005). In contrast, flow regulation plays a more important role in controlling the seasonal patterns of downstream

BGD
11, 14063–14096, 2014

pCO_2. Man-made floods are regularly released from the Xiaolangdi Dam sluice gates since 2000 to flush sediment deposition in the lower Yellow River, usually from late June every year (Wang et al., 2011; Ran et al., 2014). The deep waters supersaturated with CO_2 are first discharged, resulting in the high pCO_2 at Lijin in the wet season (Fig. 4c). Unlike the seasonal variations at Toudaoguai and Tongguan as discussed above, duration of the high pCO_2 at Lijin coincided well with the sediment flushing period, indicating the impact of flow regulation on pCO_2 dynamics. Operation of dam cascade has also modified the TAlk and pCO_2 levels at the interannual scale. Affected by upstream dams (see Fig. 1), both the TAlk and pCO_2 at Lijin in the wet season were elevated during 2011–2012, by 22 and 20 %, respectively, relative to the baseline period 1950s–1984 (Table 2). Moreover, soil conservation and vegetation restoration conducted on the Loess Plateau since the 1970s have contributed to the inter-annual changes. More organic carbon has been sequestrated as a result of these aggressive land management practices (Chen et al., 2007). Given the strong flushing and leaching effects of high-intensity rainfalls, riverine organic matter export tends to increase in the wet season, and the accompanying decomposition would increase pCO_2.

It can be concluded that the observed spatial and temporal variations of pCO_2 in the Yellow River waters were collectively affected by natural processes and human activities. In particular, human activities have changed its seasonal patterns by altering hydrological regime and carbon delivery processes. The accelerating human activity in the watershed is likely to expand the role of anthropogenic over natural factors on the pCO_2 dynamics, because stronger anthropogenic perturbations are certain to occur concerning present economic development.

4.3 Implications for CO_2 outgassing

CO_2 outgassing from river waters into the atmosphere during the carbon transport processes from land to the ocean has not been fully realized until recent years (Richey et al., 2002; Cole et al., 2007; Battin et al., 2009). Riverine pCO_2 demonstrates the intensity of CO_2 exchange across the water-air interface. Under favorable environmental

BGD
11, 14063–14096, 2014

conditions, a higher riverine pCO_2 usually represents stronger CO_2 outgassing, forming a significant carbon source for the atmosphere. However, accurate estimates of global CO_2 outgassing have been hampered by the absence of a spatially resolved pCO_2 database. Previous estimates from rivers alone involve large uncertainties, varying from 0.23 to 0.56 Gt yr^{-1} (Cole et al., 2007; Aufdenkampe et al., 2011). A latest study has even concluded that up to 1.8 Gt of carbon is annually emitted from global rivers (Raymond et al., 2013), considerably higher than was previously thought. This estimate accounts for about 32 % of the annual carbon flux transferred from terrestrial systems to inland waters (Wehrli, 2013). Given the great uncertainties, quantifying riverine pCO_2 in different orders of streams is critical to resolve a robust diagnosis of CO_2 outgassing.

With respect to the Yellow River, the lower riverine pCO_2 in the headwater region relative to the atmospheric equilibrium indicates a potential CO_2 drawdown. In comparison, the river waters in the remaining watershed are generally supersaturated with CO_2, mostly greater than 1000 µatm (Fig. 2b). With an average pCO_2 of 2810 ± 1985 µatm for the whole watershed, it is apparent that the Yellow River waters tend to act as a net carbon source for the atmosphere. Despite the uncertainties associated with outgassing calculation, recent studies on watershed-scale carbon delivery demonstrate that CO_2 efflux from rivers can substantially exceed fluvial export of carbon to the oceans (Richey et al., 2002). The Yellow River has experienced abrupt reductions in flow and TSS fluxes over the past decades and these reductions will continue in future. Its carbon fluxes reaching the ocean will therefore further decrease, and more carbon is likely to be emitted as CO_2 into the atmosphere. In view of its severe soil erosion and high TSS transport (Syvitski et al., 2005), interpretation of these fluxes in the context of climate change is of great importance for understanding the role of Yellow River in the global carbon cycle.

BGD
11, 14063–14096, 2014

5 Conclusions

The Yellow River was characterized by high alkalinity with a mean TAlk of 3665 ± 988 µmol L^{-1}. Although with significant spatial variations throughout the watershed, the TAlk remained largely stable over the study period. However, the TAlk showed seasonal variability and decreased in the wet season, suggesting the dilution effect of water discharge. Except the headwater region where the pCO_2 was lower than the atmospheric equilibrium, river waters in the remaining watershed were supersaturated with CO_2. The basin-wide mean pCO_2 was estimated at 2810 ± 1985 µatm, with the highest at 36 790 µatm. Similar to the pH and TAlk, the pCO_2 also presented significant spatial and seasonal variations. The middle reaches, mainly the Loess Plateau, showed higher pCO_2 than the upper and lower reaches, which were principally resulted from severe soil erosion and unique hydrological regime. The pCO_2 correlated positively with TSS transport when the erosion intensity was low and only the topsoils rich in organic matter were eroded. When the TSS exceeded 100 kg m^{-3} indicating the predominance of gully erosion on the Loess Plateau, the subsoils with low organic matter composition were mobilized. As a result of the reduced organic matter available for decomposition, the pCO_2 slightly decreased and then remained stable, regardless of the increasing TSS concentration.

The spatial and seasonal variations of pCO_2 were collectively controlled by natural processes and human activities. High pCO_2 in the upper and middle reaches was usually estimated from March through May when ice-melt floods transported the accumulated CO_2-laden waters in winter. Human activities, flow regulation by dams in particular, have significantly changed its seasonal pattern. While reduced turbidity and extended residence time due to dam trapping has enhanced aquatic photosynthesis and resulted in a decreased pCO_2, man-made floods through flow regulation would increase downstream pCO_2. Other anthropogenic perturbations, such as acidification, soil conservation, and agricultural irrigation, have also affected the pCO_2 dynamics. Considerably high riverine pCO_2 in the Yellow River waters with respect to the at-

BGD
11, 14063–14096, 2014

mospheric equilibrium indicates that substantial amounts of CO_2 are emitted into the atmosphere. Future efforts to estimate CO_2 outgassing are therefore urgently needed.

The Supplement related to this article is available online at doi:10.5194/bgd-11-14063-2014-supplement.

Acknowledgement. This work was supported by the Ministry of Education, Singapore (MOE2011-T2-1-101). We are grateful to the YRCC for access to the hydrological data. We thank the staff at Toudaoguai, Tongguan, and Lijin gauges for their assistance in the field.

References

Alekin, O. A., Semenov, A. D., and Skopintsev, B. A.: Handbook of Chemical Analysis of Land Waters, Gidrometeoizdat, St. Petersburg, Russia, 1973.

Alin, S. R., Rasera, M. d. F. F. L., Salimon, C. I., Richey, J. E., Holtgrieve, G. W., Krusche, A. V., and Snidvongs, A.: Physical controls on carbon dioxide transfer velocity and flux in low-gradient river systems and implications for regional carbon budgets, J. Geophys. Res., 116, G01009, doi:10.1029/2010JG001398, 2011.

American Public Health Association (APHA): Standard Methods for the Examination of Water and Wastewater, 16th edition, American Public Health Association, Washington, DC, 1985.

Aufdenkampe, A. K., Mayorga, E., Raymond, P. A., Melack, J. M., Doney, S. C., Alin, S. R., Aalto, R. E., and Yoo, K.: Riverine coupling of biogeochemical cycles between land, oceans, and atmosphere, Front Ecol. Environ., 9, 53–60, 2011.

Battin, T. J., Luyssaert, S., Kaplan, L. A., Aufdenkampe, A. K., Richter, A., and Tranvik, L. J.: The boundless carbon cycle, Nat. Geosci., 2, 598–600, 2009.

Benstead, J. P. and Leigh, D. S.: An expanded role for river networks, Nat. Geosci., 5, 678–679, 2012.

Butman, D. and Raymond, P. A.: Significant efflux of carbon dioxide from streams and rivers in the United States, Nat. Geosci., 4, 839–842, 2011.

Chen, J., Wang, F. Y., Xia, X. H., and Zhang, L. T.: Major element chemistry of the Changjiang (Yangtze River), Chem. Geol., 187, 231–255, 2002a.

BGD
11, 14063–14096, 2014

Chen, J. C., Tang, C. T., Sakura, Y. S., Kondoh, A. K., and Shen, Y. S.: Groundwater flow and geochemistry in the lower reaches of the Yellow River: a case study in Shandang Province, China, Hydrogeol. J., 10, 587–599, 2002b.

Chen, J., Wang, F., Meybeck, M., He, D., Xia, X., and Zhang, L.: Spatial and temporal analysis of water chemistry records (1958–2000) in the Huanghe (Yellow River) basin, Global Biogeochem. Cy., 19, GB3016, doi:10.1029/2004GB002325, 2005.

Chen, L. D., Gong, J., Fu, B. J., Huang, Z. L., Huang, Y. L., and Gui, L. D.: Effect of land use conversion on soil organic carbon sequestration in the loess hilly area, loess plateau of China, Ecol. Res., 22, 641–648, 2007.

Chen, S. and Ji, H.: Fuzzy optimization neural network approach for ice forecast in the Inner Mongolia Reach of the Yellow River, Hydrolog. Sci. J., 50, 319–330, 2005.

Clark, I. D. and Fritz, P.: Environmental isotopes in hydrogeology, CRC Press/Lewis Publishers, New York, 1997.

Clow, D. W. and Drever, J. I.: Weathering rates as a function of flow through an alpine soil, Chem. Geol., 132, 131–141, 1996.

Cole, J. J., Prairie, Y. T., Caraco, N. F., McDowell, W. H., Tranvik, L. J., Striegl, R. G., Duarte, C. M., Kortelainen, P., Downing, J. A., Middelburg, J. J., and Melack, J.: Plumbing the global carbon cycle: integrating inland waters into the terrestrial carbon budget, Ecosystems, 10, 171–184, 2007.

Epron, D., Farque, L., Lucot, E., and Badot, P. M.: Soil CO_2 efflux in a beech forest: dependence on soil temperature and soil water content, Ann. Sci., 56, 221–226, 1999.

Evans, W., Hales, B., and Strutton, P. G.: pCO_2 distributions and air-water CO_2 fluxes in the Columbia River estuary, Estuar. Coast. Shelf S., 117, 260–272, 2013.

Gaillardet, J., Dupre, B., Louvat, P., and Allegre, C. J.: Global silicate weathering and CO_2 consumption rates deduced from the chemistry of large rivers, Chem. Geol., 159, 3–30, 1999.

Guo, J. H., Liu, X. J., Zhang, Y., Shen, J. L., Han, W. X., Zhang, W. F., Christie, P., Goulding, K. W. T., Vitousek, P. M., and Zhang, F. S.: Significant acidification in major Chinese croplands, Science, 327, 1008–1010, 2010.

Hope, D., Palmer, S. M., Billett, M. F., and Dawson, J. J. C.: Variations in dissolved CO_2 and CH_4 in a first-order stream and catchment: an investigation of soil-stream linkages, Hydrol. Process., 18, 3255–3275, 2004.

BGD
11, 14063–14096, 2014

Hu, M., Stallard, R. F., and Edmond, J. M.: Major ion chemistry of some large Chinese rivers, Nature, 298, 550–553, 1982.
Hunt, C. W., Salisbury, J. E., and Vandemark, D.: Contribution of non-carbonate anions to total alkalinity and overestimation of pCO_2 in New England and New Brunswick rivers, Biogeosciences, 8, 3069–3076, doi:10.5194/bg-8-3069-2011, 2011.
Jones, J. B., Jr., Stanley, E. H., and Mulholland, P. J.: Long-term decline in carbon dioxide supersaturation in rivers across the contiguous United States, Geophys. Res. Lett., 30, 1495, 2003.
Kato, T., Tang, Y., Gu, S., Cui, X., Hirota, M., Du, M., Li, Y., Zhao, X., and Oikawa, T.: Carbon dioxide exchange between the atmosphere and an alpine meadow ecosystem on the Qinghai-Tibetan Plateau, China, Agr. Forest Meteorol., 124, 121–134, 2004.
Li, S., Lu, X. X., He, M., Zhou, Y., Li, L., and Ziegler, A. D.: Daily CO_2 partial pressure and CO_2 outgassing in the upper Yangtze River basin: a case study of the Longchuan River, China, J. Hydrol., 466–467, 141–150, 2012.
Li, X. D., Fu, H., Guo, D., Li, X. D., and Wan, C. G.: Partitioning soil respiration and assessing the carbon balance in a Setaria italica (L.) Beauv. Cropland on the Loess Plateau, Northern China, Soil Biol. Biochem., 42, 337–346, 2010.
Liu, Q. and Singh, V.: Effect of microtopography, slope length and gradient, and vegetative cover on overland flow through simulation, J. Hydrol. Eng., 9, 375–382, 2004.
Melack, J.: Riverine carbon dioxide release, Nat. Geosci., 4, 821–822, 2011.
Millot, R., Gaillardet, J., Dupre, B., and Allegre, C. J.: The global control of silicate weathering rates and the coupling with physical erosion: new insights from rivers of the Canadian Shield, Earth Planet. Sc. Lett., 196, 83–98, 2002.
Piòol, J. and Avila, A.: Streamwater Ph, Alkalinity, Pco2 and Discharge Relationships in Some Forested Mediterranean Catchments, J. Hydrol., 131, 205–225, 1992.
Ran, L. and Lu, X. X.: Delineation of reservoirs using remote sensing and their storage estimate: an example of the Yellow River basin, China, Hydrol. Process., 26, 1215–1229, 2012.
Ran, L., Lu, X. X., Sun, H., Han, J., Li, R., and Zhang, J.: Spatial and seasonal variability of organic carbon transport in the Yellow River, China, J. Hydrol., 498, 76–88, 2013.
Ran, L., Lu, X. X., and Xin, Z.: Erosion-induced massive organic carbon burial and carbon emission in the Yellow River basin, China, Biogeosciences, 11, 945–959, doi:10.5194/bg-11-945-2014, 2014.

BGD
11, 14063–14096, 2014

Raymond, P. A. and Cole, J. J.: Gas exchange in rivers and estuaries: choosing a gas transfer velocity, Estuaries, 24, 312–317, 2001.
Raymond, P. A. and Cole, J. J.: Increase in the export of alkalinity from North America's largest river, Science, 301, 88–91, 2003.
Raymond, P. A., Hartmann, J., Lauerwald, R., Sobek, S., McDonald, C., Hoover, M., Butman, D., Striegl, R., Mayorga, E., and Humborg, C.: Global carbon dioxide emissions from inland waters, Nature, 503, 355–359, 2013.
Richey, J. E., Melack, J. M., Aufdenkampe, A. K., Ballester, V. M., and Hess, L. L.: Outgassing from Amazonian rivers and wetlands as a large tropical source of atmospheric CO_2, Nature, 416, 617–620, 2002.
Richey, J. E.: Pathways of atmospheric CO_2 through fluvial systems, in: Scientific Committee on Problems of the Environment (SCOPE)/United Nations Environment Programme (UNEP)-The Global Carbon Cycle: Integrating Humans, Climate, and the Natural World, edited by: Field, C. B., and Raupach, M., Island Press, USA, 329–340, 2003.
Rustomji, P., Zhang, X., Hairsine, P., Zhang, L., and Zhao, J.: River sediment load and concentration responses to changes in hydrology and catchment management in the Loess Plateau region of China, Water Resour. Res., 44, W00A04, doi:10.1029/2007WR006656, 2008.
Shi, W.-Y., Tateno, R., Zhang, J.-G., Wang, Y.-L., Yamanaka, N., and Du, S.: Response of soil respiration to precipitation during the dry season in two typical forest stands in the forest-grassland transition zone of the Loess Plateau, Agr. Forest Meteorol., 151, 854–863, 2011.
Striegl, R. G., Dornblaser, M., McDonald, C., Rover, J., and Stets, E.: Carbon dioxide and methane emissions from the Yukon River system, Global Biogeochem. Cy., 26, GB0E05, doi:10.1029/2012GB004306, 2012.
Syvitski, J. P. M., Vorosmarty, C. J., Kettner, A. J., and Green, P.: Impact of humans on the flux of terrestrial sediment to the global coastal ocean, Science, 308, 376–380, 2005.
Teodoru, C. R., del Giorgio, P. A., Prairie, Y. T., and Camire, M.: Patterns in pCO_2 in boreal streams and rivers of northern Quebec, Canada, Global Biogeochem. Cy., 23, GB2012, doi:10.1029/2008GB003404 ,2009.
Tranvik, L. J., Downing, J. A., Cotner, J. B., Loiselle, S. A., Striegl, R. G., Ballatore, T. J., Dillon, P., Finlay, K., Fortino, K., Knoll, L. B., Kortelainen, P. L., Kutser, T., Larsen, S., Laurion, I., Leech, D. M., McCallister, S. L., McKnight, D. M., Melack, J. M., Overholt, E., Porter, J. A., Prairie, Y., Renwick, W. H., Roland, F., Sherman, B. S., Schindler, D. W., Sobek, S., Tremblay, A., Vanni, M. J., Verschoor, A. M., von Wachenfeldt, E., and Weyhenmeyer, G. A.:

BGD
11, 14063–14096, 2014

Lakes and reservoirs as regulators of carbon cycling and climate, Limnol. Oceanogr., 54, 2298–2314, 2009.
Wang, F. S., Wang, B. L., Liu, C. Q., Wang, Y. C., Guan, J., Liu, X. L., and Yu, Y. X.: Carbon dioxide emission from surface water in cascade reservoirs-river system on the Maotiao River, southwest of China, Atmos. Environ., 45, 3827–3834, 2011.
Wang, X., Ma, H., Li, R., Song, Z., and Wu, J.: Seasonal fluxes and source variation of organic carbon transported by two major Chinese Rivers: the Yellow River and Changjiang (Yangtze) River, Global Biogeochem. Cy., 26, GB2025, doi:10.1029/2011GB004130, 2012.
Wang, Z., Liu, G., and Xu, M.: Effect of revegetation on soil organic carbon concentration in deep soil layers in the hilly Loess Plateau of China, Acta Ecol. Sinica, 30, 3947–3952, 2010 (in Chinese).
Wehrli, B.: Biogeochemistry: conduits of the carbon cycle, Nature, 503, 346–347, 2013.
Wu, L. L., Huh, Y., Qin, J. H., Du, G., and van der Lee, S.: Chemical weathering in the Upper Huang He (Yellow River) draining the eastern Qinghai-Tibet Plateau, Geochim. Cosmochim. Ac., 69, 5279–5294, 2005.
Xu, J.: Implication of relationships among suspended sediment size, water discharge and suspended sediment concentration: the Yellow River basin, China, Catena, 49, 289–307, 2002.
Yao, G. R., Gao, Q. Z., Wang, Z. G., Huang, X. K., He, T., Zhang, Y. L., Jiao, S. L., and Ding, J.: Dynamics of CO_2 partial pressure and CO_2 outgassing in the lower reaches of the Xijiang River, a subtropical monsoon river in China, Sci. Total Environ., 376, 255–266, 2007.
Zhang, J., Huang, W. W., Létolle, R., and Jusserand, C.: Major element chemistry of the Huanghe (Yellow River), China: weathering processes and chemical fluxes, J. Hydrol., 168, 173–203, 1995.
Zhang, J., Xu, M., Wang, Z., Ma, X., and Qiu, Y.: Effects of revegetation on organic carbon storage in deep soils in hilly Loess Plateau region of Northwest China, Chinese J. Appl. Ecol., 23, 2721–2727 (in Chinese), 2012.
Zhao, M. X., Zhou, J. B., and Kalbitz, K.: Carbon mineralization and properties of water-extractable organic carbon in soils of the south Loess Plateau in China, Eur. J. Soil Biol., 44, 158–165, 2008.
Zhao, W.: The Yellow River's Sediment, Yellow River Conservancy Press, Zhengzhou, China, 807 pp., 1996.

BGD
11, 14063–14096, 2014

Table 1. pH at Luokou station during the period 1980–1984: a comparison of different data sources (arithmetic mean ± SD).

Data source	Year				
	1980	1981	1982	1983	1984
GEMS/Water Programme	8.27 ± 0.11	8.21 ± 0.21	8.10 ± 0.20	8.14 ± 0.10	8.25 ± 0.09
This study	8.11 ± 0.13	8.14 ± 0.07	8.13 ± 0.07	8.10 ± 0.03	8.09 ± 0.05
% of variation	1.93	0.85	−0.37	0.49	1.94

BGD
11, 14063–14096, 2014

Table 2. Inter-annual and seasonal differences of pH, TAlk, and pCO_2 at the three stations.

Station	Item	1950s–1984		2011–2012	
		Wet season	Dry season	Wet season	Dry season
Toudaoguai	pH	7.89	8.01	8.19	8.11
	TAlk ($\mu mol\,l^{-1}$)	3595	4091	3513	3771
	pCO_2 (μatm)	3716	2708	1580	1655
Tongguan	pH	–	–	7.91	7.72
	TAlk ($\mu mol\,l^{-1}$)	–	–	3356	4562
	pCO_2 (μatm)	–	–	2927	6016
Lijin	pH	8.18	8.19	8.23	8.28
	TAlk ($\mu mol\,l^{-1}$)	2942	3789	3576	3584
	pCO_2 (μatm)	1344	1349	1609	1132

BGD
11, 14063–14096, 2014

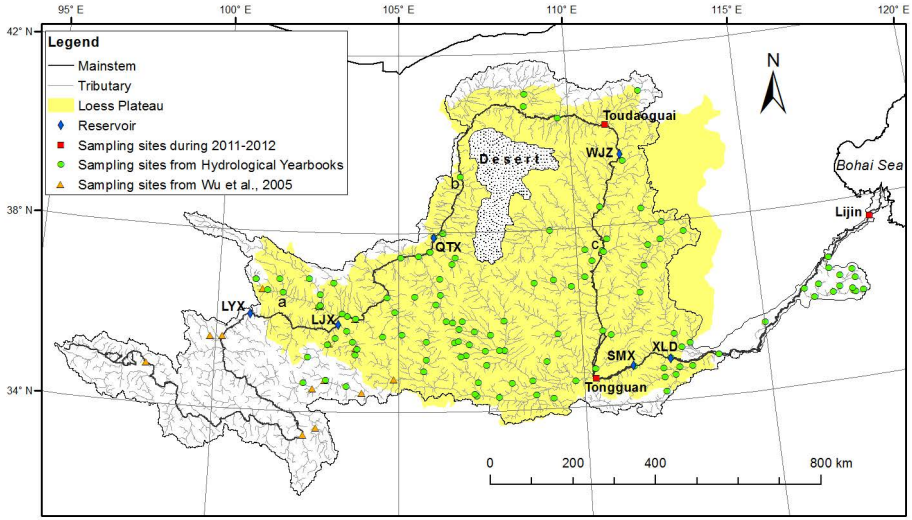

Figure 1. Location map of the sampling sites in the Yellow River watershed. Acronyms for the mainstem dams: LYX-Longyangxia since 1986; LJX-Liujiaxia since 1968; QTX-Qingtongxia since 1968; WJZ-Wanjiazhai since 1998; SMX-Sanmenxia since 1960; and XLD-Xiaolangdi since 2000.

BGD
11, 14063–14096, 2014

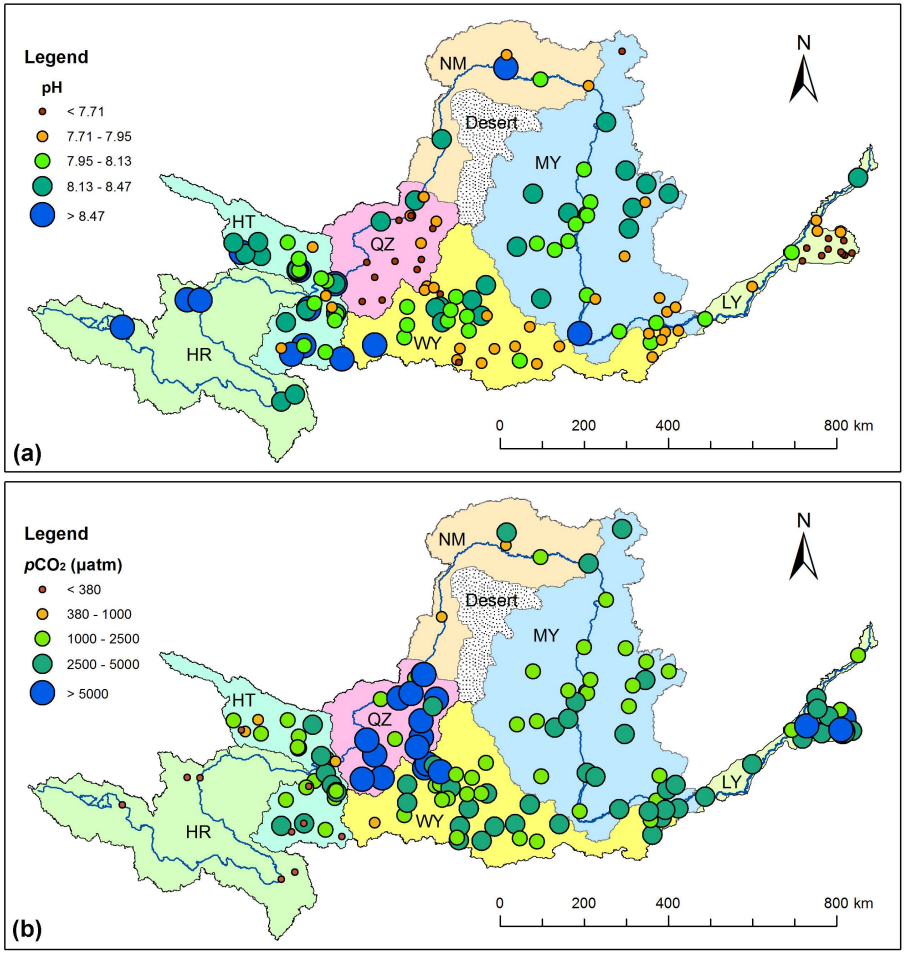

Figure 2. Spatial variations of pH **(a)** and pCO_2 **(b)** in the Yellow River basin. Acronyms were denoted in the text.

BGD
11, 14063–14096, 2014

Spatial and temporal dynamics of CO_2 partial pressure

L. Ran et al.

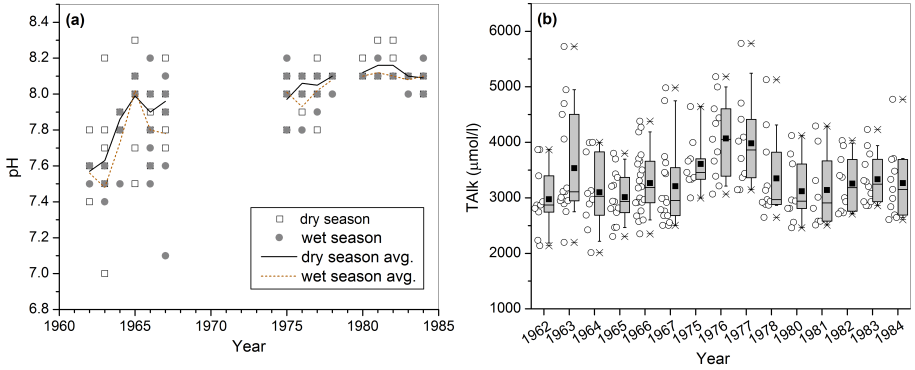

Figure 3. Seasonal comparison of pH **(a)** and box-and-whisker plot of TAlk **(b)** at Luokou station. The horizontal line is the median value, the black square is the mean value, the boxes represent the 25th to 75th percentile, the whiskers represent the 10th and 90th percentile, and the asterisks represent the maximum and minimum. Raw sampling data were added to the left.

BGD
11, 14063–14096, 2014

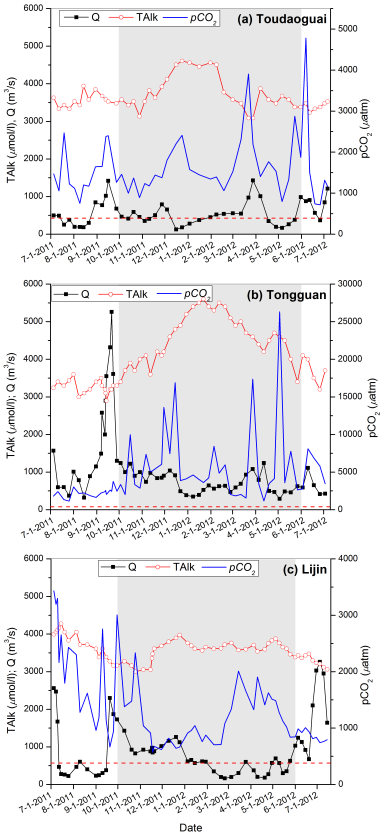

Figure 4. Weekly variations in water discharge (Q), TAlk, and pCO_2 at **(a)** Toudaoguai, **(b)** Tongguan, and **(c)** Lijin from July 2011 to July 2012. The dotted line denotes the atmospheric CO_2 equilibrium (i.e., 380 µatm) and the shaded grey represents the dry season.

BGD
11, 14063–14096, 2014

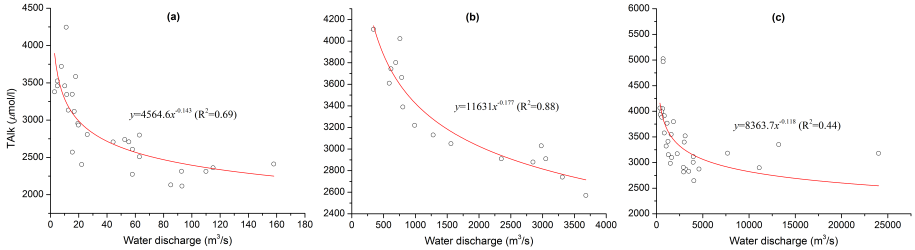

Figure 5. Dependence of TAlk on natural water discharge for different water discharge scales at typical sampling sites. **(a)** is from a tributary and **(b)** and **(c)** are from the mainstem (see Fig. 1 for locations).

BGD
11, 14063–14096, 2014

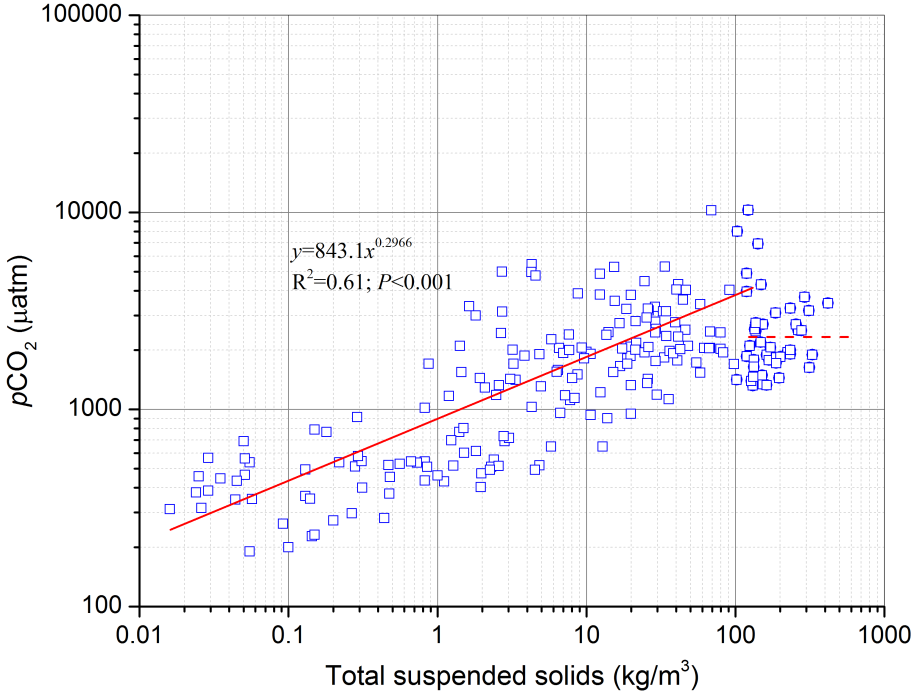

Figure 6. Relationship between total suspended solids (TSS) and pCO_2 based on measurements on the Loess Plateau.

BGD
11, 14063–14096, 2014

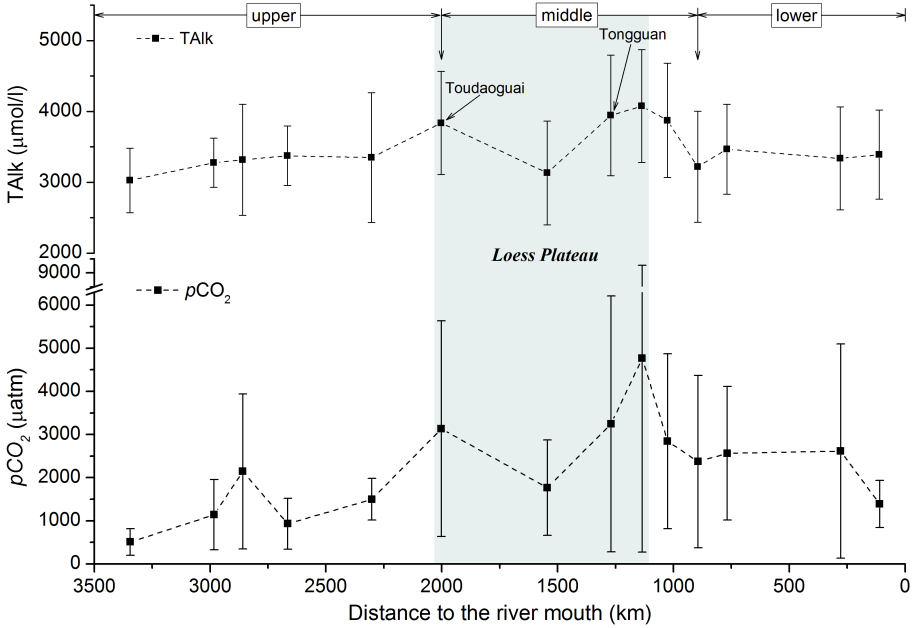

Figure 7. Downstream variations of TAlk and pCO_2 along the mainstem channel. The shaded region approximately represents the Loess Plateau. Whiskers indicate the SD.

BGD
11, 14063–14096, 2014

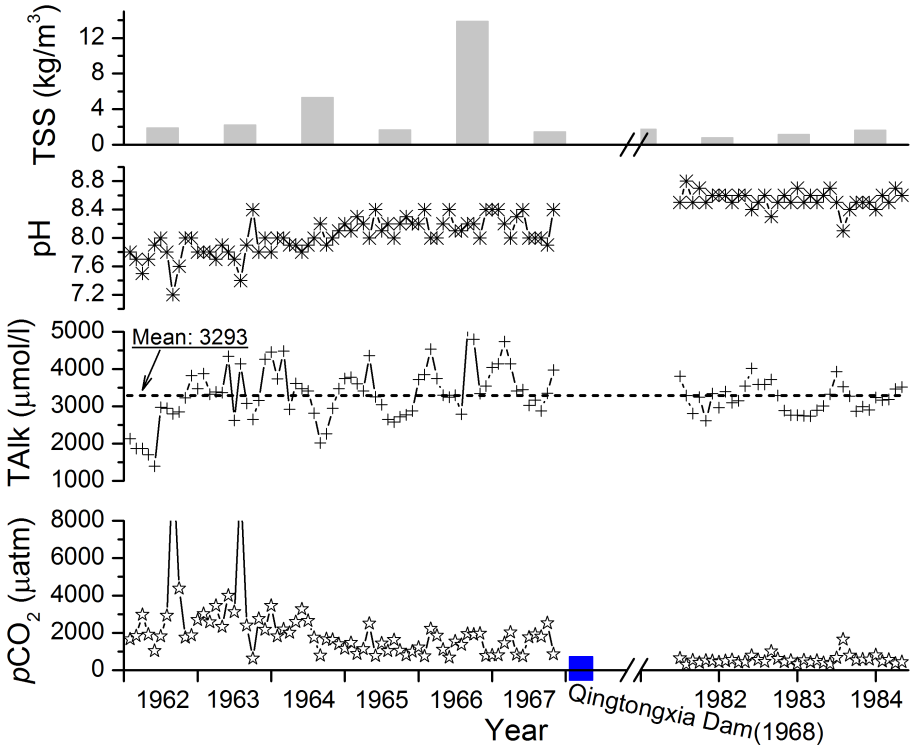

Figure 8. Impacts of Qingtongxia (QTX) dam on riverine TSS, pH, TAlk, and pCO_2. Measurements were conducted ~ 850 m downstream of the QTX dam that was built in 1968 (see Fig. 1 for location).

BGD
11, 14063–14096, 2014